JOURNAL OF THERMOPHYSICS AND HEAT TRANSFER
Vol. 20, No. 3, July–September 2006

Reduction of State-to-State Kinetics to Macroscopic Models in Hypersonic Flows

Gianpiero Colonna,* Iole Armenise,† Domenico Bruno,‡ and Mario Capitelli§
Università di Bari and CNR-IMIP, 70126 Bari, Italy

The state-to-state chemical kinetic model, which considers a kinetic equation for each vibrational state of diatomic molecules, has been applied to some supersonic flow regimes and in particular in boundary layer, nozzle expansion, and shock wave. Nonequilibrium vibrational distribution obtained in the calculations shows strong departure from equilibrium-inducing non-Arrhenius global chemical rates, which differ substantially from macroscopic rates commonly used in fluid-dynamic codes. The evolution properties of the distribution have been investigated by a zero-dimensional numerical code in controlled conditions. We are trying to obtain from zero-dimensional results the approach to find appropriate macroscopic rate models to be used in fluid-dynamic codes accounting for the vibrational nonequilibrium. A comparison of analytical fitting of the zero-dimensional data and fluid dynamic global rates has been performed.

Nomenclature

c_i	=	coefficients for the solution of the master equation
E_v	=	energy of the vth vibrational level
k	=	Boltzmann constant
k^d	=	dissociation rate constant
k^p	=	rates of the process p
N_p	=	quasi-stationary value of a given vibrational state fraction
N_v	=	population of the vth vibrational state
nD	=	space of n dimensions
P	=	pressure in homogeneous system
P_e	=	pressure at the edge of the boundary layer
P_0	=	pressure at nozzle inlet
T	=	gas temperature
T_e	=	temperature at the edge of the boundary layer
T_{eff}	=	effective temperature for rate coefficient
T_v	=	vibrational temperature based on the first vibrational level
T_{v0}	=	initial vibrational temperature
$T_{v=n}$	=	vibrational temperature based on the nth vibrational level
T_w	=	gas temperature at vehicle surface
T_0	=	temperature at nozzle inlet
t	=	time
v	=	vibrational quantum number
$[X]$	=	concentration of the X species
α	=	atomic molar fraction
α_0	=	initial atomic molar fraction
λ	=	mean free path
η	=	self-similar distance from vehicle surface
φ_v	=	collision frequency of the vth vibrational state

Presented as Paper 2005-5205 at the AIAA 38th Thermophysics Conference, Toronto, ON, Canada, 6 June–9 September 2005; received 23 June 2005; revision received 7 October 2005; accepted for publication 7 October 2005.

*Senior Researcher, Dipartimento di Chimica; gianpiero.colonna@ba.imip.cnr.it. Member AIAA.

†Researcher, Dipartimento di Chimica; iole.armenise@ba.imip.cnr.it. Member AIAA.

‡Researcher, Dipartimento di Chimica; domenico.bruno@ba.imip.cnr.it. Member AIAA.

§Professor, Dipartimento di Chimica; mario.capitelli@ba.imip.cnr.it. Fellow AIAA.

I. Introduction

STATE-TO-STATE chemical-physical models have been developed in these last years to describe the complex phenomenology occurring in hypersonic flows. These models have been inserted in different one-dimensional codes to describe the kinetics in the boundary layer of a reentering body,[1,2] in nozzle flow expansion,[3,4] and in shock waves,[5] the last via DSMC (direct simulation Monte Carlo).

The kinetics in the boundary layer as well as during nozzle expansion are characterized by strong nonequilibrium vibrational distribution functions and consequent non-Arrhenius behavior of the corresponding global chemical rates as a function of instantaneous gas temperature T.[1–4] In particular, the gas-phase recombination of atomic species pumps vibrational energy in the top of the relevant vibrational ladders thus creating long plateaux in the vibrational distribution functions. This pumping should not be confused with the Treanor's mechanism, which can also operate in this kind of flow because in the boundary layer as well as along the nozzle axis we have $T_v > T$, T_v being the vibrational temperature of the diatomic molecule, generally based on the 0-1 level population[1–4] in the state-to-state approach. A two-temperature T_v-T[6] approach hides however the long plateaux existing under these conditions.

On the other hand, in the shock-wave kinetics, we assist the sudden strong increase of gas temperature followed by the slow increase of the corresponding vibrational temperature, that is, we are in the reverse conditions $T_v < T$. Also in this case we can obtain nonequilibrium vibrational distributions caused by dissociative processes.[5]

The state-to-state vibrational kinetics is able to detail this phenomenology. However difficulties arise when coupling the state-to-state kinetics with robust two-dimensional Navier–Stokes (NS) codes, being practically impossible when coupling with three-dimensional NS codes.

To overcome this kind of difficulty, Park's approach[6–8] is commonly used; it consists in calculating the global rate coefficients, expressed by the Arrhenius equation, not at the gas temperature, but at an effective one, $T_{\text{eff}} = (T_v T)^{\frac{1}{2}}$. More recently Josyula and Bailey,[9,10] Josyula et al.,[11] and Josyula and Bailey[12] have corrected the Park's approach by modifying the relevant rates: 1) with a coefficient that is temperature dependent, which takes into account the depletion of upper vibrational levels caused by the preferential dissociation events occurring from these levels; and 2) with a coefficient that is temperature dependent, which takes into account the overpopulation of upper vibrational levels to the preferential pumping of these levels by the recombination processes.

These corrections seem to be satisfactory when the vibrational distributions do not appreciably differ from the Boltzmann ones as in the case of the shock waves. However, in rapidly expanding (nozzle) or cooling (boundary layer) flows the state-to-state kinetics

show nonequilibrium vibrational distributions dramatically far from the Boltzmann ones.

The aim of this paper is to study these strong nonequilibrium conditions indicating an approach that can be followed for determining macroscopic models, which include the main features observed by the state-to-state kinetics.

The paper is subdivided in to three sections. In the first one we discuss typical results obtained with one-dimensional codes with state-to-state kinetics for boundary layer, expanding flows, and shock waves. In the second section we will illustrate the different conditions with a zero-dimensional (time-dependent) kinetic code imitating boundary layer, nozzle, and shock-wave flows to investigate the possibility of using zero-dimensional codes to reproduce flow conditions. In the third section we will indicate a recipe to model state-to-state rates as a function of macroscopic quantities only to be used in fluid-dynamic codes.

The system investigated is a N_2/N mixture. Two chemical processes have been considered: dissociation and recombination by collisions with atoms and with molecules, in the ladder-climbing approximation.[1–4]

II. Nonequilibrium in High-Enthalpy Flows

In this section we will discuss nonequilibrium effects in one-dimensional fluid codes with state-to-state kinetics. Before analyzing the results, we want to remember that for boundary layer and nozzle flows we use the ladder-climbing model. This model consists of extending the rate coefficients of internal energy exchange processes to a pseudolevel with energy higher than the dissociation, which dissociates instantaneously. Vibrational-vibrational (VV) and vibrational-translational (VT) internal energy exchange are included in the model.[1–4] In particular VT energy exchanges for atom-molecule interaction (including the corresponding dissociation/recombination processes) consider multiquantum transitions, whereas only monoquantum transitions are considered for molecule-molecule interaction. The ladder-climbing model, used in this paper for nozzle and boundary-layer kinetics, underestimates the dissociation constants as compared with quasi-classical trajectory method.[13]

In the case of shock waves, the DSMC code adds also multiquantum molecule-molecule dissociation, disregarding the recombination process.

Two different kinds of conditions can be evidenced:

1) The first is a recombination regime where atom concentration is higher than the equilibrium one and the vibrational temperature is higher than the gas temperature. In this case the nonequilibrium is caused by the state-selective recombination, which happens mainly in highly excited vibrational levels, leading to an overpopulation of the distribution tail (boundary layer and nozzle[1–4] flows).

2) The second is a dissociation regime where the atom concentration is lower than the equilibrium one and the vibrational temperature is lower than the gas one. In this case the nonequilibrium is caused by dissociation (shock wave), resulting in depopulated distribution tails. In this model we have considered also multiquantum dissociation via the Treanor–Marrone model[14,15] (for molecule-molecule collisions) and via trajectory method for atom-molecule collisions.[16]

In hypersonic boundary layers the temperature gradient, caused by surface temperature lower than in the shock layer, causes a density gradient, and therefore transport and kinetic processes work together leading to chemical and vibrational nonequilibrium. This is an example of flow in recombination regime. The Navier–Stokes equations have been simplified separating the flow in two self-similar coordinates, one longitudinal and the other one η perpendicular to the surface, obtaining an equation that depends only on η. The details of the model we use to simulate boundary layers are deeply discussed in Refs. 1 and 2. In this work we have considered as boundary conditions a noncatalytic surface at temperature $T_w = 1000$ K while the boundary-layer edge temperature is $T_e = 7000$ K and local thermodynamic equilibrium is supposed. Two pressures, assumed constant through the boundary layer, 10^3 N/m^2 or 10^5 N/m^2 have been considered.

The vibrational distributions have been compared for the two considered pressures in three different positions in the boundary layer (see Fig. 1), at the surface ($\eta = 0$), at the outer edge of the boundary layer ($\eta = 8$) and in a intermediate point ($\eta = 1.62$) where the temperature gradient is high. In both conditions the distributions show an increase of the tails and the cooling at low energy levels while approaching the surface. The differences between the two pressure conditions are maximum at the surface. The high-pressure case gives colder low energy distributions and less populated tails because of the increase of the frequencies of VT collitions with the pressure. Close to the surface the presence of thermal nonequilibrium can be observed (see Fig. 2), where we have compared the gas and the vibrational temperatures, calculated from the first two vibrational levels by the equation

$$T_v = \frac{E_1 - E_0}{k[\ell_n(N_0) - \ell_n(N_1)]} \tag{1}$$

under the assumption of a Boltzmann vibrational distribution. Close to the wall the vibrational temperature is higher than the gas

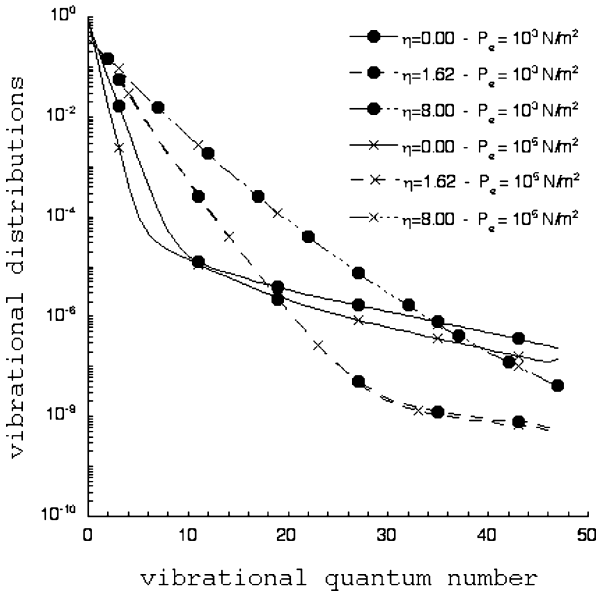

Fig. 1 Vibrational distributions in the boundary layer, obtained including all of the kinetic processes for different η ($\eta = 0$ is on the surface and $\eta = 8$ is at the edge), compared at two different pressures P.

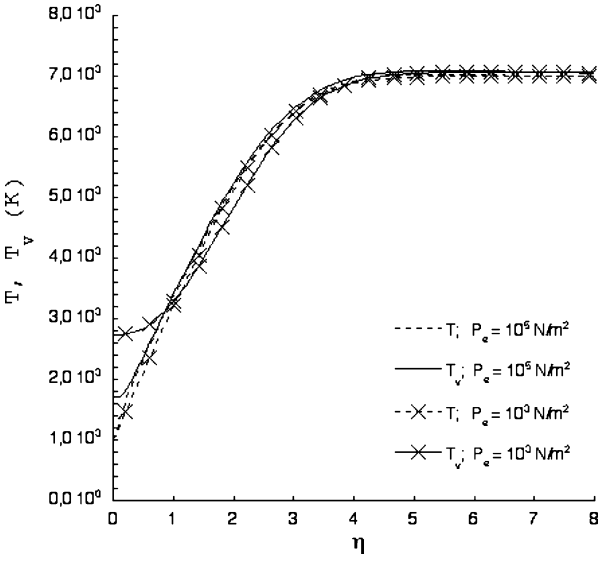

Fig. 2 Gas T and vibrational T_v temperatures in the boundary layer obtained including all of the kinetic processes compared at two different pressures P.

temperature, and at low pressure T_v freezes at higher values because of the slower kinetics.

Nonequilibrium distributions are mainly caused by the recombination processes,[1,2] as can be observed comparing Figs. 1 and 3, where the vibrational distributions have been obtained neglecting the recombination processes: in this case the overpopulated tails disappear showing Boltzmann-like distributions. However, departures from equilibrium can be observed (see Fig. 4); comparing the wall distributions calculated at the two given pressures, with the Boltzmann distributions calculated at the local T, at the local T_v, and at $T_{\text{eff}} = (T_v T)^{\frac{1}{2}}$ the distributions calculated with the state-to-state approach present non-Boltzmann character: the vibrational-distribution-function (VDF) tails are always higher than the Boltzmann distributions calculated at the local vibrational temperature. (Note that in the boundary layer we have $T_v > T_{\text{eff}} > T$.)

Note also that the VV up-pumping mechanism plays a negligible role in the formation of the plateau in Fig. 1 because of the small difference of T_v and T temperature as well as the presence of atomic nitrogen close to the surface.

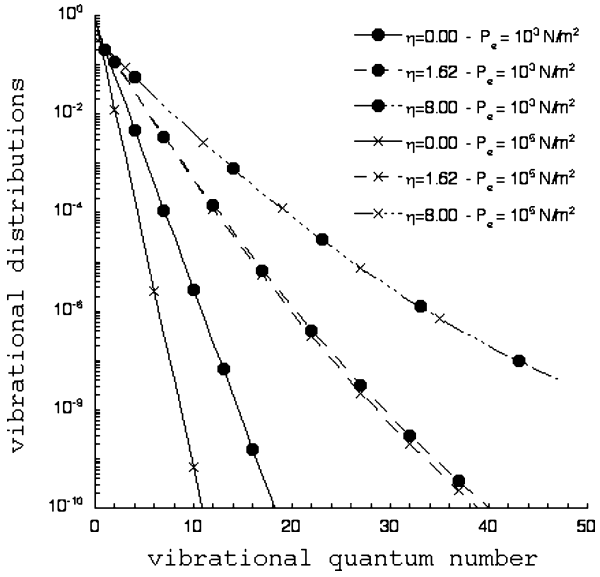

Fig. 3 Vibrational distributions in the boundary layer, obtained neglecting recombination processes for different η ($\eta = 0$ is on the surface and $\eta = 8$ is at the edge), compared at two different pressures P.

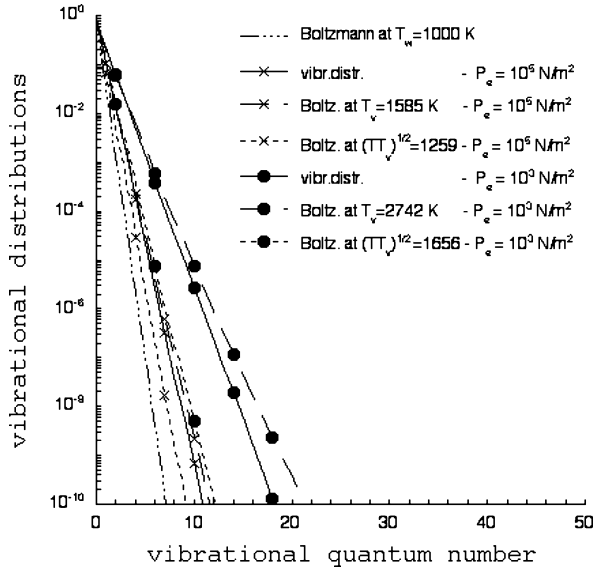

Fig. 4 Boundary-layer–surface vibrational distributions calculated with the state-to-state model, obtained neglecting the recombination process, and Boltzmann distributions at different temperatures, both at $P = 10^3$ and 10^5 N/m^2.

To understand the role of the nonequilibrium on the dissociation processes, their rate constants k^d are approximated by the ladder-climbing model of the VT processes. Two dissociation processes are considered: by $N_2 - N_2$ molecular collisions (VTm) and by $N_2 - N$ atomic collisions (VTa). In Figs. 5 and 6, the rate coefficients have been plotted as a function of $1/T_v$. When the recombination processes have been neglected (symbols), Arrhenius-like dissociation constants correspond to Boltzmann-like distributions.

The case in which all of the processes have been included shows strong departure from the Arrhenius law: the lower values of $1/T_v$ correspond to the boundary-layer edge. In this region the system is close to the local thermodynamic equilibrium, and the VDF are very close to a Boltzmann distributions; hence, the rates follow the Arrhenius trend as in the case where the recombination is neglected. Approaching the surface, the distributions strongly depart from a Boltzmann, and the rate coefficients show an anomalous trend: the rates increase while the vibrational temperature decreases. In previous works[1–4] the rates were reported as a function of the reverse of the local gas temperature showing similar behaviors to those in Figs. 5 and 6.

The last point of the rate coefficient presents an anomalous trend; it suddenly changes close to the wall. This result is the consequence

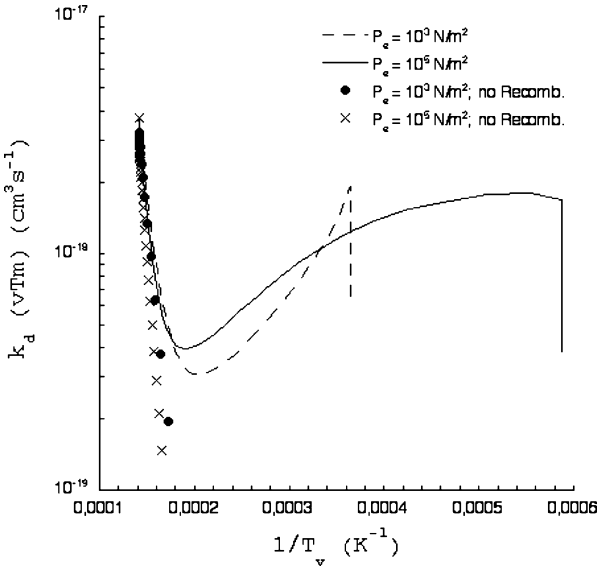

Fig. 5 Boundary-layer–dissociation constants caused by VT processes by $N_2 - N_2$ collisions, obtained including and neglecting recombination.

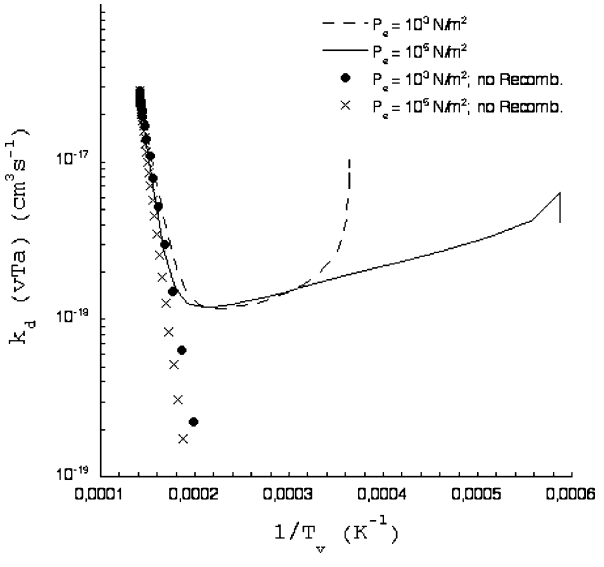

Fig. 6 Boundary-layer–dissociation constants caused by VT processes by $N_2 - N$ collisions, obtained including and neglecting recombination.

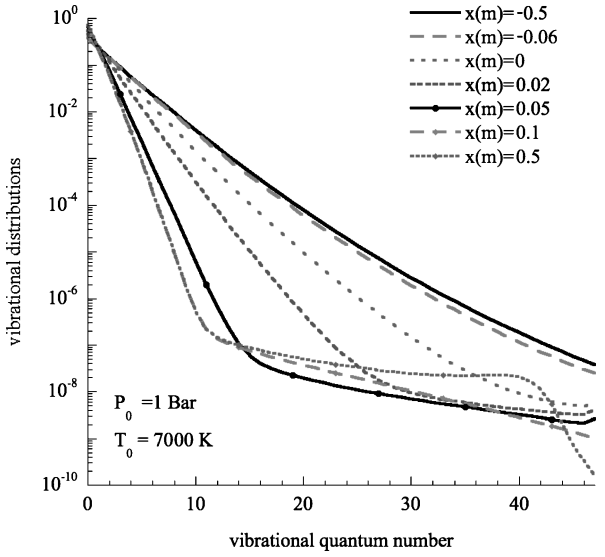

Fig. 7 Vibrational distributions along the nozzle axis. $X = 0$ is the throat position.

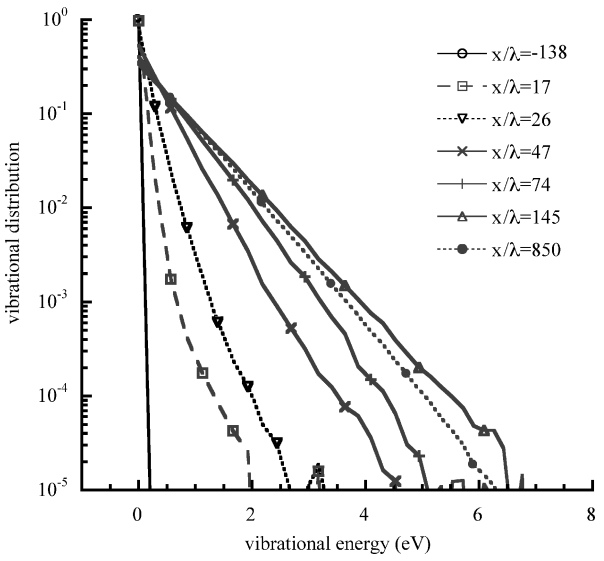

Fig. 8 Vibrational distributions in a shock wave for different positions from the shock ($x = 0$ is the shock position). l is the mean free path.

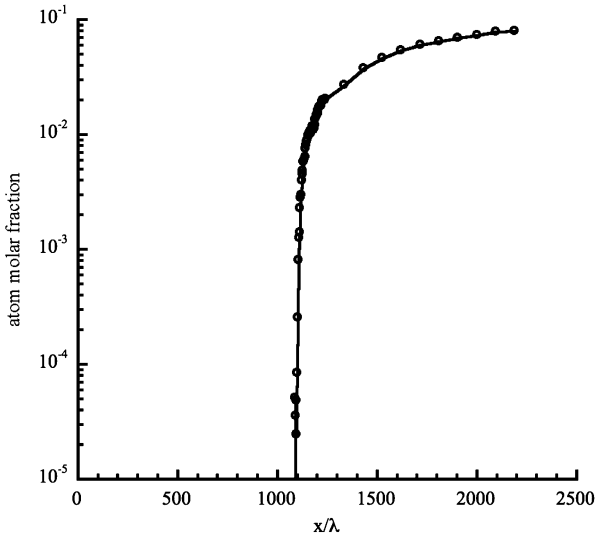

Fig. 9 Atom molar fraction profile along shock wave.

of different wall boundary conditions for species mass fractions and for the gas temperature. Because of the noncatalytic wall, the mass fractions have a null derivative at the wall. On the contrary the temperature decreases rapidly close to the surface because the wall temperature is supposed to be constant. Therefore, although close to the wall the distributions are constant, the decreasing temperature makes the state to state as well as the global rates decrease because of their dependence on the gas temperature.

This result demonstrates that modified Arrhenius rates do not reproduce the calculated global rates because they are determined by the distribution tail while the vibrational temperature represents only the low energy distribution. Moreover their behaviors do not depend only on the temperatures, but also on other quantities such as pressure and boundary conditions.

Another flow system, which works in recombination regime, is the supersonic nozzle expansion.[3,4] The main difference between boundary layer and nozzle flows is that in the first one the pressure is constant, but in the nozzle the pressure changes many orders of magnitude passing from the inlet to the exit. Nevertheless, the distributions (see Fig. 7) show the same long tails that are observed in the boundary layer. The distributions are Boltzmann at the nozzle inlet, and as the flow passes the throat the temperature decreases rapidly and the atoms recombine producing in the vibrational distributions the characteristic tails. The pressure reduction makes the vibrational temperature practically frozen to the nozzle exit while the distribution tail is still relaxing. As a consequence of non equilibrium distributions, non-Arrhenius trends have been observed also in this case,[3,4] demonstranting uniform behaviors for recombination flow regimes. Also in this case the VV up-pumping mechanism is decreased by the presence of atomic nitrogen.

We have investigated relaxation properties also in a shock wave using a DSMC code.[5] With this approach it is possible to observe also translational nonequilibrium, and the reference length is the mean free path λ. The shock wave is wide only a few λ, and the gas temperature reaches its maximum just after it. On the contrary, vibrational and rotational temperatures and gas composition need a longer distance from the shock front to reach the equilibrium values. The nonequilibrium generated in the shock layer is completely different from nozzle and boundary-layer flows being the system in dissociation regime. The first relevant process is the VT pumping that warms up the distribution from low-lying levels to the tails (see Fig. 8). This mechanism is also important for the dissociation process. In fact, as observed in Fig. 9, the atomic molar fraction is negligible until the vibrational distribution is sufficiently high. This happens in spite of the fact that the DSMC code consider also multiquantum dissociation for $N_2 + N_2$ collisions following the Treanor–Marrone model.[14,15]

Anyway, the distributions depart weakly from a Boltzmann; therefore, the rates are almost Arrhenius (see Fig. 10). The higher $1/T$ values ($>1.6 \times 10^{-4}$) correspond to the region before the shock, where statistical errors are large. The lower $1/T$ values correspond to the region downstream of the shock where the dissociation is effective. The statistical errors are intrinsic in DSMC models, and the distribution tails present strong noise; therefore, the method is not adequate to analyze small departures from the Boltzmann distribution. At this purpose a zero-dimensional master equation code, in which the only independent variable is the time, can be a more suitable tool for investigating nonequilibrium in dissociation regime.

III. Nonequilibrium in Homogeneous Systems

The analysis of nonequilibrium in supersonic flows is not simple because all of the macroscopic quantities (temperature, pressure, compositions, etc.) are coupled to each other and to the vibrational distributions. In homogeneous kinetics (depending only on time) it is possible to calculate the evolution of species concentration keeping constant some quantities such as pressure and temperature, working in more controlled conditions. Moreover it is possible to simulate relaxation conditions similar to those met in supersonic flow conditions. In particular we investigate two cases: recombination regimes (nozzle and boundary layer) and dissociation (shock wave).

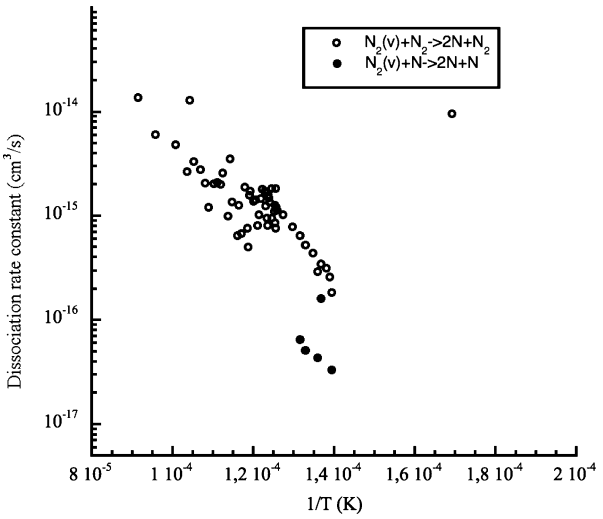

Fig. 10 Dissociation rate constants along the shock wave as a function of the reverse of the temperature.

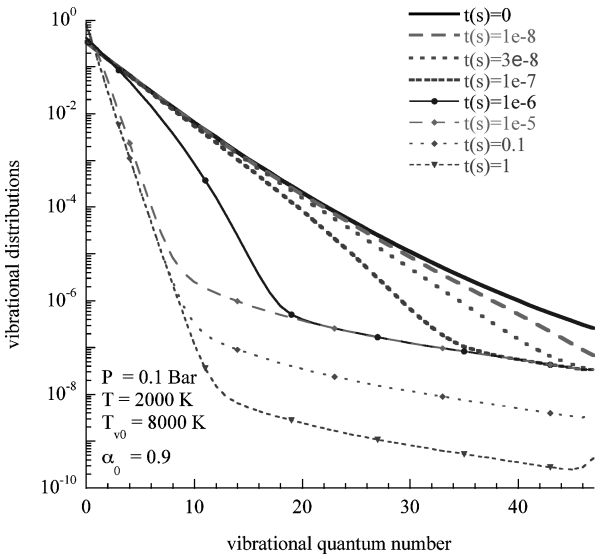

Fig. 11 Time evolution of the vibrational distribution function of N_2 molecules in recombination regime.

There are two kinds of parameters in the simulation. The first class of data consists of those that are constant during all of the simulation: gas temperature T and pressure P. The second group of parameters consists of those chosen as initial conditions, and they are the initial vibrational temperature T_{v0} and the initial atomic molar fraction (α_0). These quantities can change during the simulation.

In this section we want to use a zero-dimensional code to analyze the kinetic relaxation of the inhomogeneous gas in different regimes, comparing the results with those showed in the preceding section, to understand if zero-dimensional kinetics can be applied to investigate appropriate flow conditions. In particular we will focus on the recombination and dissociation regimes met in the fluid-dynamic systems just studied. Note that the numerical results are obtained using the ladder-climbing model described earlier.

A. Recombination regime

In the recombination regime the gas passes from high-temperature to low-temperature conditions. This is the case of supersonic nozzle flows and boundary layer of reentry vehicles. In our conditions we suppose the gas to be partially dissociated at the beginning, with a high vibrational temperature. Then we suppose to decrease instantaneously the gas temperature, and we start to investigate the relaxation processes of the mixture. The vibrational distribution cools down, passing through nonequilibrium states.

The relaxation presents some common characteristics that do not depend on the chosen conditions. In Fig. 11 we have reported the evolution of the vibrational distributions.

At the beginning of the simulation, we have a Boltzmann distribution at the given vibrational temperature T_{v0}. The distributions start relaxing from the tail (high energy levels). The distribution tail decreases until it reaches a quasi-stationary condition. After that, the low energy distribution ($v < 15$) starts cooling down obtaining an L-shape distribution for $t = 10^{-5}$ s. Then, for longer times the distribution tail decreases again trying to reach the equilibrium distribution at the gas temperature.

The quasi-stationary conditions can be observed better in Fig. 12, where we have compared the relative population of the last level and the molar fraction of atoms α. The quasi-stationary value of the last level distribution N_p depends on the pressure, and it is reached before the atomic molar fraction changes. The time evolution of the system can be divided in three stages. First of all the last level rapidly reaches the quasi-stationary phase, keeping constant the vibrational temperature and the atomic molar fractions (compare with Fig. 11). Then the vibrational temperature decreases while the population of the last vibrational level and the atomic molar fractions are constant. In the third stage the vibrational temperature is constant, whereas atomic molar fraction and the population of the last level change contemporarily.

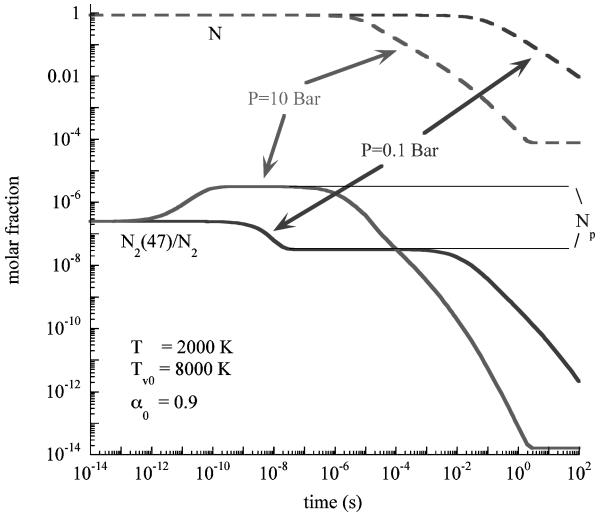

Fig. 12 Evolution of atomic molar fraction and the relative population of the last vibrational level ($v = 47$), for two different pressures in recombination regime. N_p is the population of the last level in the quasi-stationary phase.

To understand what determines the quasi-stationary condition in the distribution tail, we consider the relaxation kinetics of the last vibrational level. The time evolution of a level is determined by the kinetic equation

$$\frac{\mathrm{d}N_2(v)}{\mathrm{d}t} = \text{gain} - \text{loss}$$

$$\text{gain} = k_r^a(v,T)N^3 + k_r^m(v,T)N^2N_2$$

$$\text{loss} = k_{vT}^a(v,T)NN_2(v) + k_{vT}^m(v,T)N_2N_2(v) \qquad (2)$$

where in the recombination regime the gain is mainly caused by the recombination and the loss to VT collisions. In the quasi-stationary phase we can consider that atomic molar fraction is constant so that the only quantity that changes in the preceding equation is the population of the last vibrational level. As a consequence, Eq. (2) can be written as

$$\frac{\mathrm{d}}{\mathrm{d}t}\frac{N_2(v)}{N_2} = a - b\frac{N_2(v)}{N_2} \qquad (3)$$

where a and b are functions of T, P, and α. The kinetic equation (2) has an analytical solution given by

$$\frac{N_2(v,t)}{N_2} = \left[\frac{N_2(v,0)}{N_2} - \frac{a}{b}\right]\exp(-bt) + \frac{a}{b} \tag{4}$$

The quasi-stationary solution is given by the ratio a/b. The same result can be obtained equating gain and loss terms and writing all of the quantities as a function of T, P, α; we obtain the equation

$$N_p(v) = \frac{P}{kT(1-\alpha)}\frac{k_r^a(v,T)\alpha^3 + k_r^m(v,T)\alpha^2(1-\alpha)}{k_{vT}^a(v,T)\alpha + k_{vT}^m(v,T)(1-\alpha)} \tag{5}$$

The characteristic time necessary to reach the quasi-stationary solution is the reverse of the parameter b in Eq. (5) given by

$$b = P/kT\left[k_{vT}^a(v,T)\alpha + k_{vT}^m(v,T)(1-\alpha)\right] \tag{6}$$

From Eqs. (4–6) we have an idea of what is the quasi-stationary solution and the time needed to reach it. This result is approximated because some processes have been neglected in the analytical model (such as VV, the gain caused by VT processes and dissociation), but in the recombination regime and far from equilibrium should be accurate, especially for the last levels. In general, VV processes can be important for expanding flows when the vibrational temperature overcomes the translational one. However, in presence of atomic species the role of VV collisions is weakened,[1–5] so that the vibrational distribution depends mainly on the recombination and VT processes.

In Fig. 13 we have reported the value of the quasi-stationary population N_p of the last vibrational level ($v = 47$) as a function of the pressure. The calculated points have been fitted by a power law, confirming the prediction of Eq. (5).

It is interesting to analyze if the dependence of the quasi-stationary population of the vibrational state $v = 47$ has a regular dependence on the atomic molar fraction (see Fig. 14). The data have been fitted by a third-order polynomial.

We have investigated the behavior of the last vibrational state because the global rate coefficient, which should be used in macroscopic kinetics, is mainly determined by the distribution tail and therefore should have the similar properties of the population of the last vibrational level. A consideration can be done looking at the figures in this paragraph: the quasi-stationary population of the last vibrational level does not depend on the vibrational temperature and also the characteristic time needed to reach that value. In fact when the distribution tail changes, the vibrational temperature is constant (see Fig. 11), and during the quasi-stationary phase for the last vibrational level the vibrational temperature changes. These observations are in agreement with the results of Ref. 17.

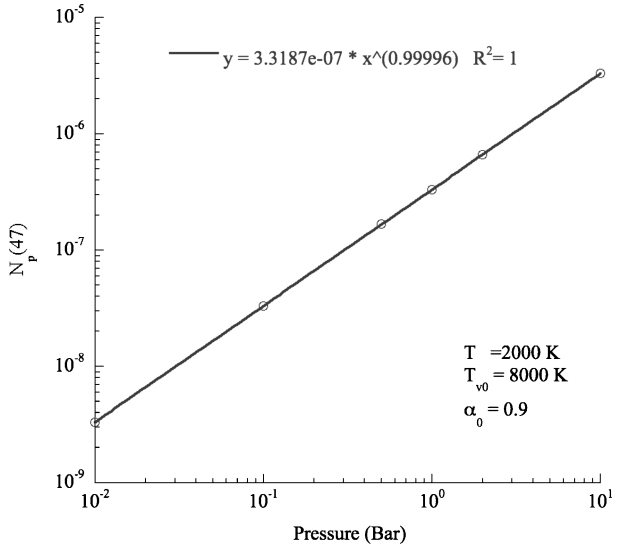

Fig. 13 Quasi-stationary value of the last vibrational level as a function of the gas pressure.

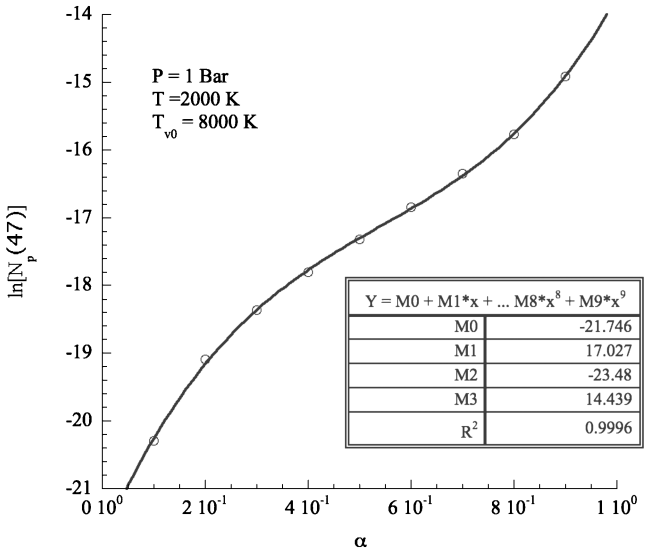

Fig. 14 Logarithm of the quasi-stationary value of the last vibrational level as a function of the atomic molar fraction.

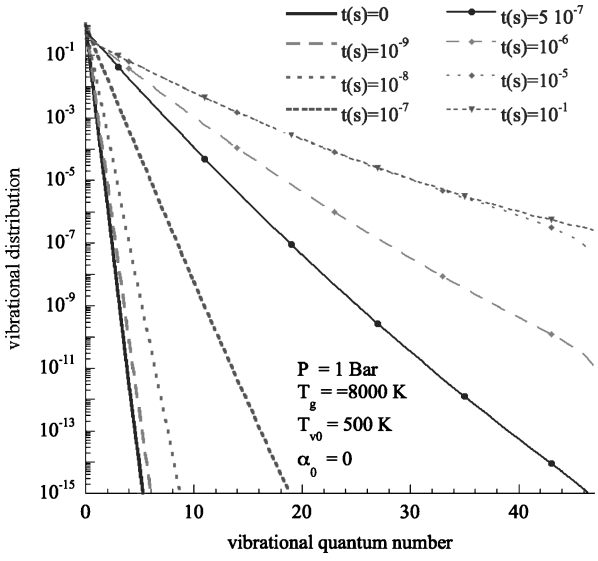

Fig. 15 Time evolution of vibrational distribution of N_2 calculated in dissociation regime.

B. Dissociation Regime

With homogeneous kinetics it is possible to reproduce also conditions met in shock tubes. In these conditions we have a low-pressure cold gas with supersonic velocity that through a shock wave changes instantaneously the temperature and pressure, decreasing rapidly the flow speed. Then the internal degree of freedom and the chemistry relax to reach the equilibrium conditions.

To simulate shock-wave conditions, we consider a pure N_2 gas with a cold vibrational distribution in a high-temperature ambient. In the simulation, $N_2(v) - N_2$ multiquantum transitions are neglected so that one can expect an underestimation of the global dissociation rates, especially at high temperature.

Therefore, before nitrogen atoms appear, the high levels of the vibrational ladder must be populated. When the population of the last vibrational level reaches a value appreciably high, the dissociation starts, according to the ladder-climbing model here used. Insertion of dissociation channel from every vibrational level (in particular low-lying ones) by molecule-molecule collisions, as in the atom-molecule collisions, should increase the global dissociation rates. Unfortunatly, these transitions are poorly known at the moment, so that their role cannot be seriously extimated. Figures 15 and 16 report the time evolution of the vibrational distribution and molar

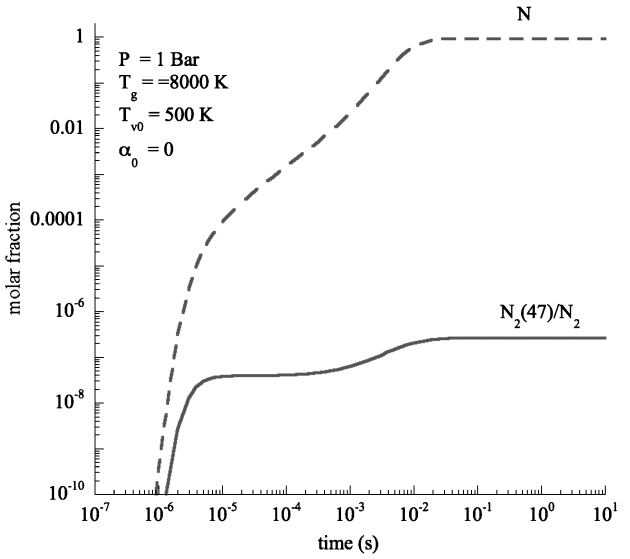

Fig. 16 Evolution of atomic molar fraction and the relative population of the last vibrational level ($v = 47$) in recombination regime.

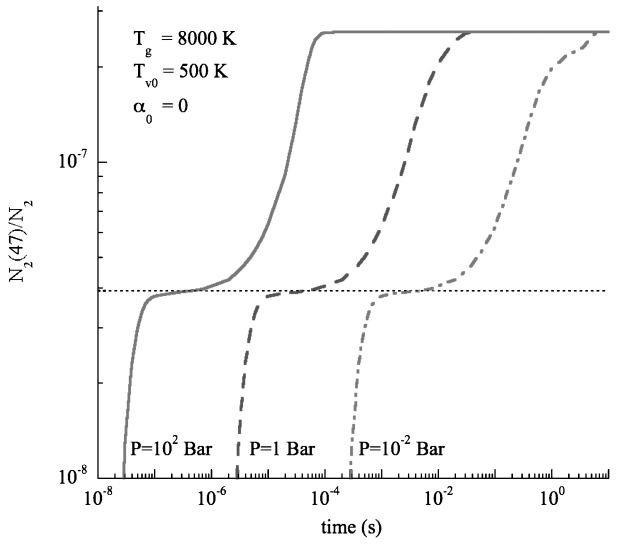

Fig. 17 Evolution of the population of the last vibrational level ($v = 47$) for three different pressures in recombination regime. N_p is the population of the last level in the quasi-stationary phase.

fraction of atoms, molecules, and the fraction of molecules in the last vibrational levels $[N_2(47)/N_2]$. It can be observed that the distribution is almost Boltzmann with small deviations for high levels. In this case the multitemperature approach could be quite accurate. The atom molar fraction becomes appreciable after $t = 10^{-6}$ s as a consequence of the ladder-climbing mechanism. Around $t = 10^{-5}$ s a quasi-stationary population of the last vibrational level is observed. This observation can be the basis for building a simplified model. Considering that the dominant process is the $N_2 - N_2$ VT up pumping (VV processes can be in fact neglected when $T > T_v$), it is possible to make an approximate analysis of the solution. Such processes consider only monoquantum transitions; therefore, it is possible to write a master equation like Eq. (2), where the gain and loss are given by

$$\text{gain} = k^{vTm}_{v-1,v} N_2 N_2 (v-1), \qquad \text{loss} = k^{vTm}_{v,v+1} N_2 N_2 (v) \tag{7}$$

The analytical solution of this equation is more complicated because it depends on the entire distribution. Under the approximation that the population N_0 of the ground state is constant and considering the collision frequency

$$\varphi_v = k^{vTm}_{v,v+1} N_2 \tag{8}$$

the time evolution of the population N_v of each vibrational level can be calculated by a recursion method obtaining

$$N_v(t) = c_0 \frac{\varphi_0}{\varphi_v} + \sum_{n=1}^{v-1} c_n e^{-\varphi_n t} \prod_{i=n}^{v-1} \frac{\varphi_i}{\varphi_{i+1} - \varphi_n} + c_v e^{-\varphi_v t} \tag{9}$$

where the constants c are calculated from the initial conditions. The limit to infinity of Eq. (9) gives the value of the quasi-stationary distribution

$$N_v^{qs} = c_0 \frac{\varphi_0}{\varphi_v} = N_0 \frac{k^{vTm}_{0,1}}{k^{vTm}_{v,v+1}} \tag{10}$$

where for the last level, the rate to the denominator is the dissociation one.

The quasi-stationary distribution depends only on the population of the ground state, and it does not depend on the pressure. This result has been verified also numerically, comparing the time evolution of the fraction of the last vibrational level for different pressures (see Fig. 17). The quasi-stationary values have been evidenced with a horizontal line.

This solution is valid until the atom concentration is negligible. In fact in Fig. 16 a variation of the slope of the atomic molar fraction with the growing of the population of the last vibrational level can be observed. This is a consequence of other processes, such as $N_2 + N$ collisions. We have also neglected the reverse processes that in quasi-stationary state can give a contribution, but in our opinion their contribution is small until the atom production is appreciable. The dissociation regime is more complex than the recombination one, involving many processes and parameters; therefore, further investigation is needed to try to build a macroscopic model based on the state-to-state behaviors of the distributions.

IV. Modeling Global Rates

As observed in the preceding section, the rate coefficients used in the multitemperature approach are not in agreement with the results obtained by the homogeneous chemical kinetics in the state-to-state approach. This result was also obtained in one dimensional models,[1–4] where endothermic rate coefficients show, for low temperature, large departures from the Arrhenius shape.

In this section we want to verify if the homogeneous approach can be used to determine global rates to be used in fluid dynamic system and if it is possible, from these data, to find a mathematical expression that can reproduce the global rates obtained in one-dimensional codes. In this case we focus our attention in the recombination regime. In the preceding section we have found the quantities that affect the last level of the vibrational ladder. The global rate coefficients are calculated summing the state-to-state rates over the vibrational distribution

$$R_p(T, \ldots) = \sum_v k_v^p(T) \frac{N_2(v, T, \ldots)}{N_2} \tag{11}$$

where the dots stand for all of the unknown parameters. In the case of dissociation and in general for all of the endothermic processes the state selective rates increase with the vibrational quantum number and in general are effective only from the higher vibrational levels.

For example, in the case of $N_2 + N_2$ dissociation the state-to-state (ladder-climbing) model considers the dissociation effective only from the last level, whereas the $N_2 + N$ dissociation take place from any level. This last rate is linearly correlated with the last vibrational level (see Fig. 18) with small deviations at low gas pressure.

This result can be explained by the following considerations. The rate of $N_2 + N$ dissociation is effective mainly from the vibrational tails that are correlated with the last vibrational level. Therefore, following the behavior of the last vibrational level could be a good approach to determine the shape of the vibrational tail and therefore

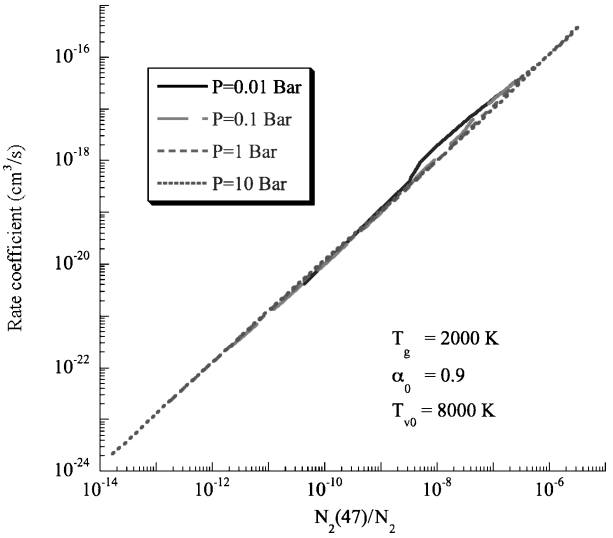

Fig. 18 Global rate coefficient of the process $N_2 + N -> 3N$ as a function of the population of the last vibrational level for different gas pressures.

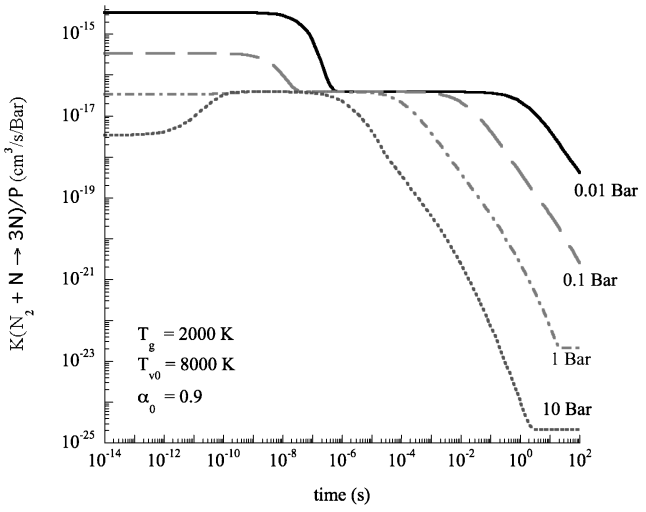

Fig. 19 Time evolution of the global rate coefficient of the process $N_2 + N -> 3N$ divided by the pressure for different gas pressures.

of the rate coefficients. As a consequence, all of the relations between the last vibrational level, discussed in the preceding section, are valid for the global rate coefficients.

In Fig. 19 we have reported the time evolution of the global rate coefficient for different pressures. It is possible to observe the rapid relaxation of the ratio K/P to a quasi-stationary level, which is independent from the gas pressure, and then it shows a slower relaxation to the equilibrium values. In this last phase, the rate coefficient does not depend directly on time, but it follows the time changes of the ambient parameters, and in our case, being constant pressure and the gas temperature, it is related to the molar fraction of atomic nitrogen as can be observed in Fig. 20, where we have reported the rate coefficient of the process $N_2 + N = 3N$ divided by the gas pressure as a function of the atomic molar fraction. One can observe that the curve is very regular except for molar fraction values =0.9, where the rates change while the atomic molar fraction is constant. These points correspond to the first relaxation phase (see Fig. 12), where the last level population changes while the molar fraction of atomic nitrogen is constant.

From these results a consideration can be done about the dependence of the global rates on relevant macroscopic quantities. We have two different behaviors: for short time, the rate depends directly on time, and its evolution is given by an equation similar to Eq. (3) (in differential form) and Eq. (4) (in analytical form) because of the connection with the last vibrational level, until it reaches the

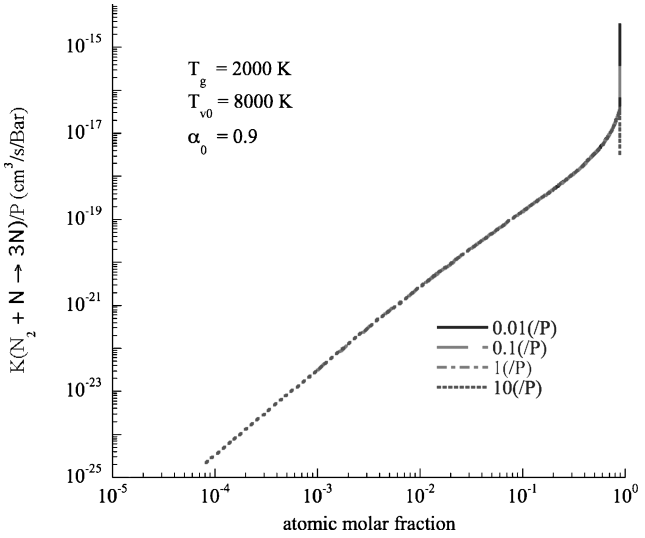

Fig. 20 Global rate coefficient divided by the pressure of the process $N_2 + N -> 3N$ as a function of the atomic nitrogen molar fraction, for different gas pressures.

quasi-stationary state; after that it can be expressed as a function of some macroscopic quantities that in the specific case are P, T, α.

At this stage we want to prove if these results obtained in a time-dependent homogeneous system can be exported to fluid-dynamic systems. We have considered two fluid-dynamic systems that are in recombination regimes. The first example considered is the gas cooling in the boundary layer of hypersonic reentry blunt body. At the external edge of the boundary layer (the shock layer), we have an high temperature ($T_e = 7000$ K), and the gas is in equilibrium at such temperature (partially dissociated), while the wall is cooled ($T_w = 1000$ K). The pressure in the boundary layer is constant ($P = 1$ bar), and in this case we have neglected catalytic processes on the surface. The second example is the expansion into vacuum of an heated gas ($T_0 = 7000$ K) at high pressure ($P_0 = 1$ bar) through a converging-diverging nozzle. At the nozzle exit the gas temperature is below 300 K, and the pressure is a few tens of Pascal. In both systems, recombination is an important process, and strong nonequilibrium distributions have been observed.[1–4] As a consequence, the global dissociation rates show large departures from the Arrhenius trend.

To compare the homogeneous results with the fluid-dynamic ones, we have fitted the homogeneous rates calculated for different conditions with a multivariate function:

$$\log(K_d) = f[\log(\alpha), T, P] = \log(P) + \frac{\sum_{i=0}^{4} \mathrm{pol}_i[6, \log(\alpha)]T^i}{\log(\alpha)^{2q}}$$

$$\mathrm{pol}_i[n, x] = \sum_{j=0}^{n-1} a_{ij} x^j \qquad (12)$$

We must point out that this is a very simple function that can be improved. But the purpose of this comparison is to understand if, at least qualitatively, it is possible to reproduce the data calculated in flow conditions with the homogeneous results.

In Figs. 21 and 22 we have reported the function in Eq. (12) using the parameter calculated by the least-square method applied to the homogeneous results and compared with the rate coefficients calculated in the boundary layer (Fig. 21) and in nozzle flow (Fig. 22).

The agreement is qualitatively good, reproducing the trend in both conditions. The discrepancies can be caused by two factors. The first one is that the polynomial fitting function in not very suitable because can produce spurious oscillations. The second reason can be that in some regions the quasi-stationary approximation is not verified, and therefore a time-dependent approach is necessary.

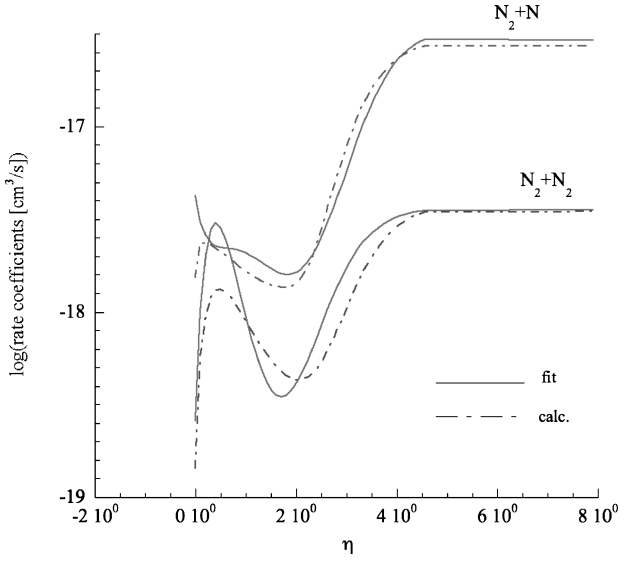

Fig. 21 Logarithm of the global dissociation rates, calculated in the boundary layer of a reentry body as a function of the Lees–Dorodtsin[1] coordinate from the surface, compared with the function obtained by fitting homogeneous results.

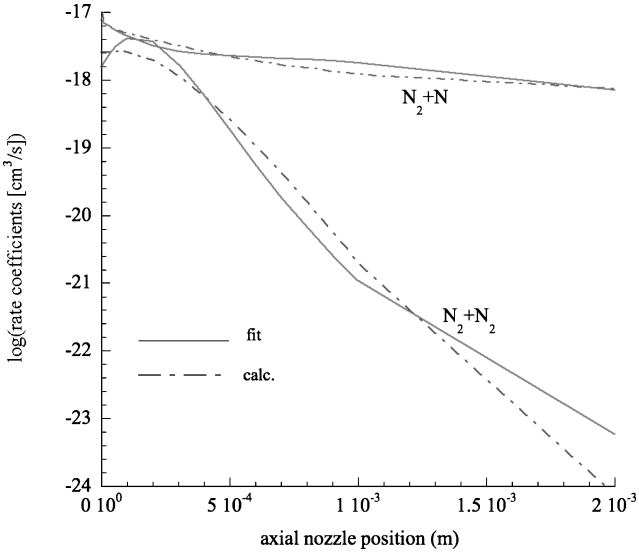

Fig. 22 Logarithm of the dissociation rate coefficients, calculated in a nozzle expansion as a function of the axial distance from the throat, compared with the function obtained by fitting homogeneous results.

These results shows that it is possible to find analytical models different from the traditional multitemperature relation[6,7] for global rate coefficients.

A different approach could be achieved making use of the quasi-stationary state (QSS) collisional radiative model of Bates et al.[18] for atomic plasmas. According to this model, one writes a linear system of master equations for the electronically excited states of an atomic species solving it by the QSS approach, which consists in putting the temporal derivative of the population density equal to zero for all internal levels but the ground state. The resulting deviations from the Boltzmann behavior depend on the electron density and temperature and on the ground state population density.

Sharma et al.[8] were able to develop the QSS model for describing the dissociation/recombination processes in molecular nitrogen. His QSS rates, which depend only on the temperature, are usefull especially when the deviations of the vibrational distributions from the Boltzmann one are small. This kind of result was obtained by Sharma et al.[8] by numerical experiments miming the dissociation and recombination processes, starting from and arriving to equilibrium conditions.

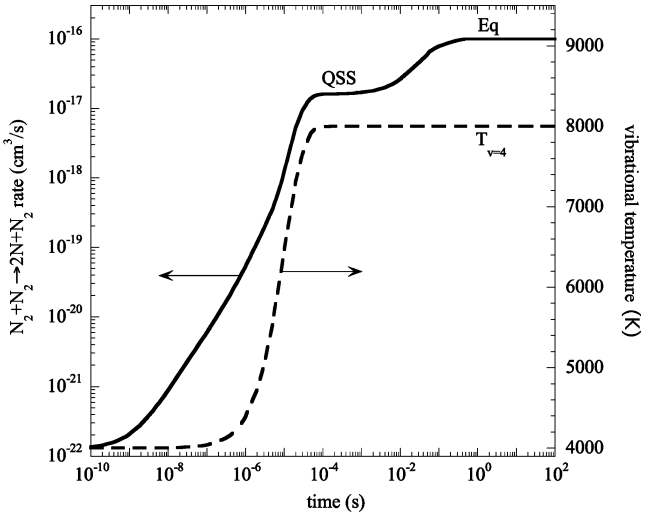

Fig. 23 Dissociation rates and vibrational temperature of the $v = 4$ vibrational level as a function of time in dissociative regime. The initial conditions are $T_v = 4000$ K; $T = 8000$ K; $[N_2] = 10^{17}$ cm^{-3}; $[N] = 2.19 \times 10^{14}$ cm^{-3}, reproducing conditions in Ref. 8.

In particular they followed the relaxation of the vibrational distribution and of the dissociation-recombination constants after an abrupt increase of the gas temperature from 4000 to 8000 K (dissociative regime) as well as an abrupt decrease of the gas temperature from 6000 to 4000 K (recombination regime) We have run our zero-dimensional code for the two case studies considered by Sharma et al. In general our results differ from those reported by Sharma et al. because of the different choice of the rates. In particular in the recombination process with N_2 as third body, we populate only the last vibrational level contrary to the multiquantum transition considered in Ref. 8.

For the dissociative regime, we report in Fig. 23 the time evolution of the global dissociation rate coefficients ($N_2 + N_2 \rightarrow 2N + N_2$) and of the vibrational temperature based on $v = 4$ level.[8] A qualitative agreement can be noted by comparing these results with the corresponding one reported by Sharma et al.[8] (In particular $T_{v=4}$ of Fig. 2 in Ref. 8 and the "exact" dissociation rates of Fig. 5 in Ref. 8.) Our dissociation rates are lower than those of Ref. 8 because of the neglection in our model of the $N_2 + N_2$ dissociation from all vibrational levels. Another difference is that we can define two dissociation constants, one in the absence of the recombination process (first plateaux in Fig. 23, marked with "QSS") corresponding to the quasi-steady-state solution (QSS), and the other one in the presence of the recombination process (see the second plateaux marked with "Eq"), corresponding to the equilibrium rate.

For the recombination regime, we report in Fig. 24 the same quantities as in Fig. 23. These curves can be compared with the corresponding results reported in Figs. 10 and 11 of Ref. 8. The differences in this case are much more pronounced. In particular our $T_{v=4}$ values monotonically decrease from 6000 to 4000 K while values in Ref. 8 reach a maximum value of 14,000 K in μs timescale. At the same time our dissociation constants decrease up to a stable plateaux and start again to decrease following atom concentration. On the contrary, the exact results in Ref. 8 show a maximum absent in our calculation. The different behavior can be ascribed once again to different sets of rates used in the two simulation.

Note also that the strong nonequilibrium vibrational distributions observed in our one-dimensional calculations (boundary layer and nozzle flow) are the result not only of the vibrational kinetics but also on the extreme nonequilibrium flow conditions met in the numerical experiments. Reduction of the actual rates to the forms suggested by Park[6,7] and Sharma et al.[8] also under strong nonequilibrium conditions should facilitate the introduction of this phenomenology in robust Navier–Stokes code. Study in this direction is in progress in our laboratory.

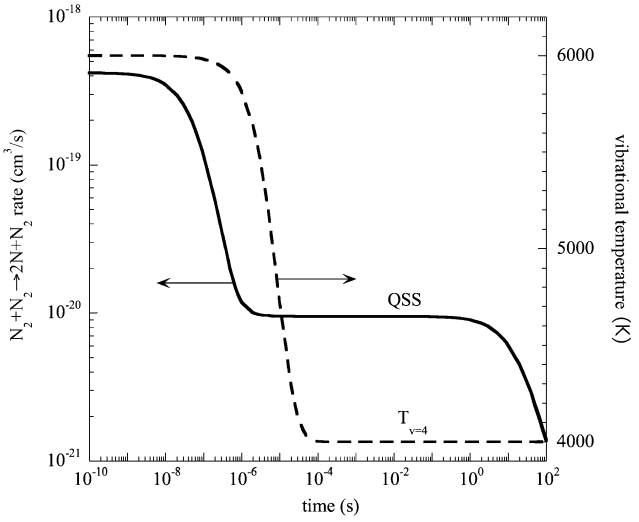

Fig. 24 Dissociation rates and vibrational temperature of the $v = 4$ vibrational level as a function of time in recombination regime. The initial conditions are $T_v = 6000$ K; $T = 4000$ K; $[N_2] = 10^{17}$ cm^{-3}; $[N] = 2.35 \times 10^{16}$ cm^{-3}, reproducing conditions in Ref. 8.

V. Conclusions

In this paper we have investigated the importance of nonequilibrium distributions in high-enthalpy flow conditions. Recombination produces strong deviations of the vibrational distributions from the Boltzmann behavior. We have also proved that it is possible to qualitatively reproduce the behaviors of the vibrational distributions in flow conditions (boundary layer, nozzle, and shock wave) using a zero-dimensional code (time-dependent master equations). Analytical solutions of the master equations have been obtained under certain approximations valid in particular conditions (recombination and dissociation regimes) that can be met in high-enthalpy flows. We have shown that the relevant parameters that affect the global rates are pressure, gas temperature, and atomic molar fraction, while the vibrational temperature seems to be practically ineffective, except for the shock wave. The results obtained by the zero-dimensional code have been compared with the results obtained by fluid-dynamic codes in recombination regime obtaining a satisfactory agreement. This shows the possibility of using the homogeneous state-to-state kinetic model to build a macroscopic kinetic model for fluid-dynamic codes. We must underline that the results obtained are strictly connected to the considered model. Different mixtures (air) or different state-to-state rates can give different results, even if the general behavior should be very close to that one presented in this paper. Anyway the method used here to build macroscopic models can be extended to more complex systems.

Acknowledgments

This paper has been partially supported by Agenzia Spaziale Italiana under Contract ASI-CAST and by MIUR under contract FIRB RBAU01H8FW_003.

References

[1]Armenise, I., Capitelli, M., and Gorse, C., "Nitrogen Nonequilibrium Vibrational Distributions and Non-Arrhenius Dissociation Constants in Hypersonic Boundary Layers," *Journal of Thermophysics and Heat Transfer*, Vol. 12, No. 1, 1998, pp. 45–51.

[2]Armenise, I., and Capitelli, M., "State to State Vibrational Kinetics in the Boundary Layer of Entering Body in Earth Atmosphere: Particle Distributions and Chemical Kinetics," *Plasma Sources, Science and Technology*, Vol. 14, No. 2, 2005, pp. S9–S17.

[3]Colonna, G., Tuttafesta, M., Capitelli, M., and Giordano, D., "Non-Arrhenius NO Formation Rates in One-Dimensional Nozzle Airflow," *Journal of Thermophysics and Heat Transfer*, Vol. 13, No. 3, 1999, pp. 372–375.

[4]Colonna, G., Esposito, F., and Capitelli, M., "The Role of State-Selected Recombination Rates in Supersonic Nozzle Expansion," AIAA Paper, 2003-3645, June 2003.

[5]Bruno, D., Capitelli, M., Esposito, F., Longo, S., and Minelli, P., "Direct Simulation of Non-Equilibrium Kinetics Under Shock Conditions in Nitrogen," *Chemical Physics Letters*, Vol. 360, No. 1-2, 2002, pp. 31–37.

[6]Park, C., *Nonequilibrium Hypersonic Aerothermodynamics*, Wiley, New York, 1990, Chap. 3.

[7]Park, C., "A Review of Reaction Rates in High Temperature Air," AIAA Paper 89-1740, June 1989.

[8]Sharma, S. P., Huo, W. M., and Park, C., "Rate Parameters for Coupled Vibration-Dissociation in a Generalized SSH Approximation," *Journal of Thermophysics and Heat Transfer*, Vol. 6, No. 1, 1992, pp. 9–21.

[9]Josyula, E., and Bailey, W. F., "Vibration-Dissociation Coupling Using Master Equations in Nonequilibrium Hypersonic Blunt-Body Flow," *Journal of Thermophysics and Heat Transfer*, Vol. 15, No. 2, 2001, pp. 157–167.

[10]Josyula, E., and Bailey, W. F., "Vibration-Dissociation Coupling Model for Hypersonic Blunt-Body Flow," *AIAA Journal*, Vol. 41, No. 8, 2003, pp. 1611–1613.

[11]Josyula, E., Bailey, W. F., and Xu, K., "Nonequilibrium Relaxation in High Speed Flows," AIAA Paper 2004-2468, June 2004.

[12]Josyula, E., and Bailey, W. F., "Governing Equations for Weakly Ionized Plasma Flowfield of Aerospace Vehicles," *Journal of Spacecraft and Rockets*, Vol. 40, No. 6, 2003, pp. 845–857.

[13]Esposito, F., Capitelli, M., and Gorse, C., "Quasi-Classical Dynamics and Vibrational Kinetics of $N + N_2(v)$ System," *Chemical Physics*, Vol. 257, No. 2-3, 2000, pp. 193–202.

[14]Marrone, P. V., and Treanor, C., "Chemical Relaxation with Preferential Dissociation from Excited Vibrational Levels," *Physics of Fluids*, Vol. 6, No. 9, 1963, p. 1022.

[15]Treanor, C., and Marrone, P. V., "Effect of Dissociation on the Rate of Vibrational Relaxation," *Physics of Fluids*, Vol. 5, No. 9, 1962, p. 1215.

[16]Capitelli, M., Colonna, G., and Esposito, F., "On the Coupling of Vibrational Relaxation with the Dissociation-Recombination Kinetics: from Dynamics to Aerospace Applications," *Journal of Physical Chemistry A*, Vol. 108, No. 41, 2004, pp. 8930–8934.

[17]Cacciatore, M., Capitelli, M., and Dilonardo, M., "Non Equilibrium Vibrational Population and Dissociation Rates of Oxygen in Electrical Discharges: the Role of Atoms and of the Recombination Process," *Beiträge aus der Plasma Physik*, Vol. 18, No. 5, 1978, pp. 279–299.

[18]Bates, D. R., and Kingston, A. E., "Recombination and Energy Balance in a Decaying Plasma. 2. He-He^+-e Plasma," *Proceedings of the Royal Society of London A*, Vol. 279, No. 1376, 1964, pp. 32–38.